Accurate Simulation of Doping-Dependent Silicide Contact Resistance Using Nano-contact Test Structure for 22nm-node and Beyond

Seong-Dong Kim [a], Emre Alptekin [a], Sameer Jain [a], Huiling Shang [a], Andreas Scholze [b] Stephen Furkay [b], Dong-Ick Lee [a], Christian Lavoie [c], Paul Solomon [c]
IBM SRDC, [a]Hopewell Junction, NY, [b]Essex Junction, VT, [c]IBM Research Division, Yorktown Heights, NY, USA
sdkim@us.ibm.com

Mark Raymond
GLOBALFOUNDRIES, Inc.
Albany, NY, USA

Abstract— **Doping-dependent (D-D) Schottky contact model is accurately calibrated in the context of three-dimensional (3D) TCAD simulations to experimental active doping levels at the silicide interface using a novel nano-contact test structure. Sophisticated contact resistance modeling including non-uniform doping-dependent specific contact resistivity along the silicide interface is demonstrated to be a key requirement for accurate simulation of contact resistance behavior in the sub-50nm contact length regime. Activation level requirements for mid-gap and low-barrier silicide contact cases are addressed for next-generation silicide contact technology development.**

Keywords- TCAD; CMOS; Schottky contact model; external resistanc; specific contact resistivity; Schottky barrier height; silicide contact

I. INTRODUCTION

Reduction of silicide contact resistance (R_{co}) represents one of the key challenges with respect to realization of high performance CMOS technologies beyond 22nm node. External resistance (R_{ext}) drastically increases with aggressive contact length scaling below the contact transfer length, L_t [1-2], hence the focus of next-generation technology development is on mitigating contact resistance contribution in total on-resistance. The dependence of R_{ext} on i) silicide contact shape and ii) non-uniform, doping-dependent contact resistivity is investigated for sub-100nm gate-pitches via advanced contact resistivity modeling. A doping-dependent Schottky contact model is calibrated in the context of 3D TCAD simulations to experimental data derived from nano-contact test structures. Subsequent simulations addressed ITRS requirements on i) active doping levels and ii) silicide Schottky barrier height (SBH) for next-generation silicide contact technology development. The impact of contact resistivity on R_{ext} is also characterized by using R_{ext} component extraction method via quasi-Fermi potential distributions.

II. CONTACT RESISTANCE WITH SCALING

This work has been supported by the independent Bulk CMOS and SOI technology development projects at the IBM Microelectronics, Div. Semiconductor Research & Development Center, Hopewell Junction, NY 12533.

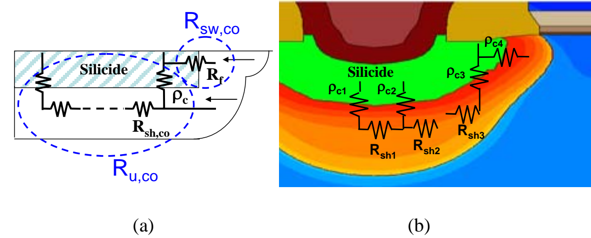

(a) (b)

Figure 1. (a) Simple contact resistance components having front sidewall contact resistance ($R_{sw,co}$) and planar contact ($R_{u,co}$) and (b) the actual complex silicide shape which is modeled as a network of complex resistance components having non-uniform contact resistivity along the silicide interface and non-uniform sheet resistance beneath.

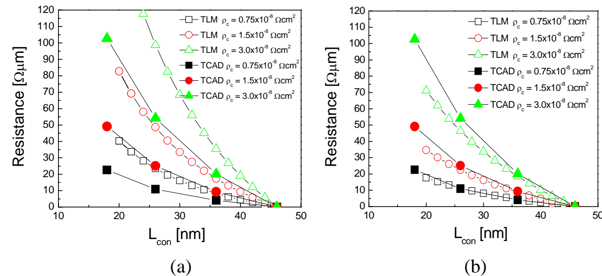

(a) (b)

Figure 2. Comparison of contact resistance increase with contact length scaling between 1D TLM and TCAD for (a) TLM without $R_{sw,co}$ component and (b) TLM including $R_{sw,co}$ component. TLM without the $R_{sw,co}$ component overestimated contact resistance, whereas inclusion of the $R_{sw,co}$ component yielded reasonable agreement with TCAD results.

Silicide contact resistance is very sensitive to the silicide topology, location and active interface doping level in the sub-50nm contact length regime. It can be modeled as a network of complex resistance components having non-uniform contact resistivity along the silicide interface and non-uniform sheet resistance beneath as illustrated in Fig.1. The significance of the sidewall contact ($R_{sw,co}$) component is demonstrated by comparing resistance variations with contact length scaling,

ISBN 978-0-615-71756-2

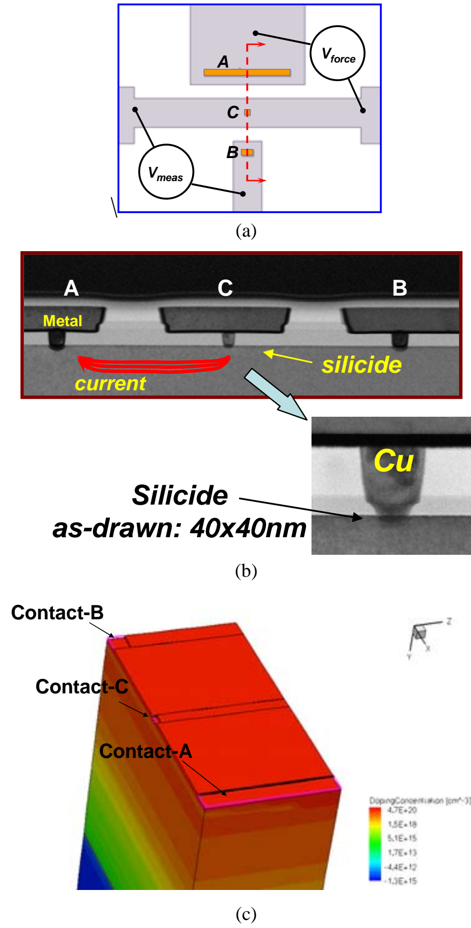

Figure 3. (a) Schematic top view of nano-contact test structure to accurately measure specific contact resistivity, (b) cross sectional TEM image of test contact structure with NiPt silicide contact, and (c) 3D nano-contact simulation structure (half device is shown).

between the 1D transmission line model (TLM) and TCAD simulations as shown in Fig. 2. TLM without the $R_{sw,co}$ component overestimates contact resistance, whereas inclusion of the $R_{sw,co}$ component yielded reasonable agreement with TCAD results with the assumption of constant contact resistivity. Decreasing contact length, L_{con} drives an increase in the relative contribution of $R_{sw,co}$ and hence the need to account for non-uniform contact resistivity. Results are therefore generated based on the D-D contact model.

III. 3D Simulation of Nano-contact Test Structure

NiPt silicide contacts are fabricated with a novel nano-contact test structure [3], in which contact hole lengths below 100nm are defined by e-beam lithography and 22nm CMOS process. The schematic top view of nano-contact test structure, the cross-sectional TEM image and 3D nano-contact simulation structure are shown in Fig. 3 (a) (b) and (c), respectively. Accurate extractions of contact resistivity enable calibration of the D-D contact model in our 3D simulations.

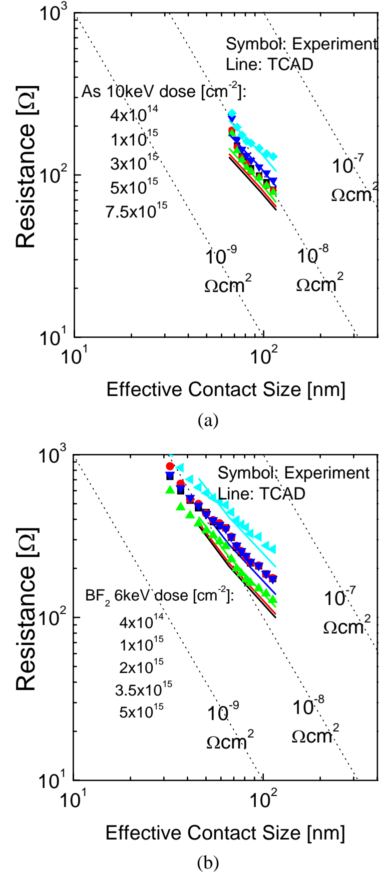

Figure 4. Measured and modeled contact resistance with various implantation doses as a function of effective contact size for (a) As implanted S/D contact, and (b) BF_2 implanted S/D contact.

Active doping levels in excess of $3\sim4\times10^{20}cm^{-3}$ are achieved with As and BF_2 extensions (EXT) and source/drain (S/D) implants of various doses, followed by high temperature RTA annealing. Physical contact sizes, critically important for contact resistivity estimation, are determined via TEM images as shown in Fig. 3 (b). The process flow and measurement details have been previously reported in [3].

The Synopsys Sentaurus TCAD tools are employed for all structure generation and simulation operations [4]. Process and device simulation model parameters are calibrated through SIMS and sheet resistance (R_{sh}) measurements on ultra-shallow junction hardware where the chemical profiles are matched to SIMS profiles and the activation levels are tuned by Rsh measurements. The active doping profiles of interface are assumed to be unchanged during silicidation. Model parameters for contact resistance are fitted to measured data and are consistent with reported NiSi silicide data [e.g., 5].

IV. Results and Discussion

The calibrated contact resistances reflect various As and BF_2 doses, and are in reasonable agreement with measured data

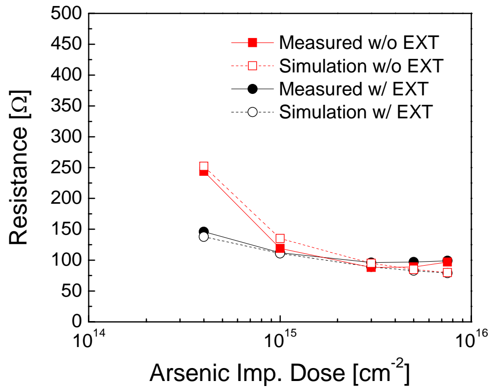

(a)

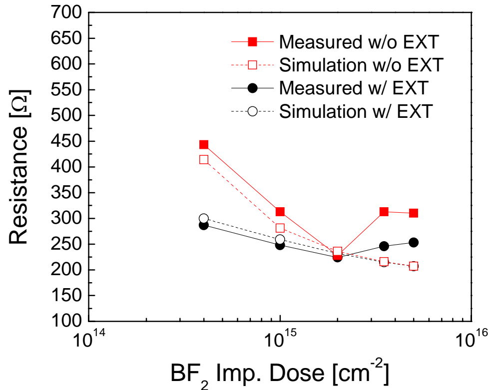

(b)

Figure 5. Measured and modeled contact resistance as a function of implantation dose at the same effective contact hole (L_{eff}= 68nm) for (a) As implanted S/D contact, and (b) BF2 implanted S/D contact.

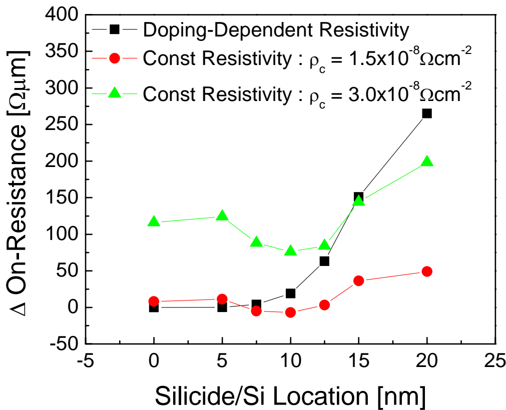

Figure 6. Contact resistance behavior as a function of vertical silicide location with different contact resistivity modeling. D-D contact model shows substantially different behavior, compared to a conventional constant resistivity model exhibiting significant R_{on} degradation with deeper silicide interface location, and higher sensitivity to silicide thickness.

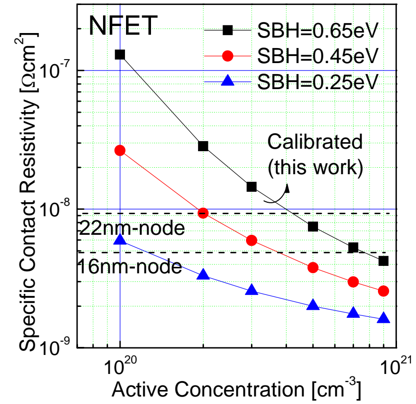

(a)

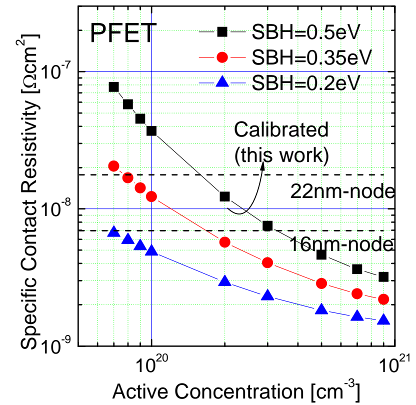

(b)

Figure 7. Specific contact resistivity projection as a function of active doping level and SBH resulted from calibrated D-D model. 2010 updated ITRS projections for ρ_c are inserted [6]. ρ_c near or below 22nm node target, is possible via the combination of midgap silicide and millisecond anneal, but low-barrier silicide or SBH reduction engineering in conjunction with high activation is indicated for 16nm technology and beyond.

(e.g., series spreading resistance dependency, $\propto L^{-1}$, contact resistance dependency $\propto L^{-2}$). Fig. 4 illustrates effective contact size dependencies, which also show reasonable agreement with experiment data [3]. It can also be deduced from Fig. 4 that the extracted specific contact resistance, ρ_c can be reduced below 10^{-8} Ω-cm^2 by enhancing activation levels. Good agreement is also obtained for with- and without-EXT implantation cases, with the exception of very high BF_2 dose cases, which exhibited deactivation as shown in Fig. 5.

The calibrated D-D contact model is applied to NFET on-resistance (R_{on}) simulations. Fig. 6 shows simulated contact resistance behavior as a function of vertical silicide location at S/D diffusion with respect to contact resistivity modeling. Substantially different behavior, compared to a conventional constant resistivity model, is observed. Significant R_{on} degradation with deeper silicide interface location, and higher sensitivity to silicide thickness, is noted. Lowering of S/D

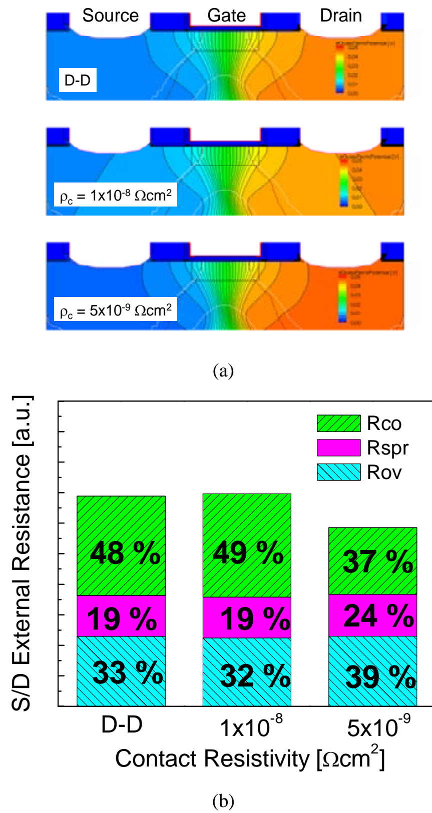

Figure 8. (a) NFET electron quasi-Fermi potential distributions with contact resistivity and (b) R_{ext} component breakdown using electron quasi-Fermi potential distribution analysis. R_{co} is comparable to other R_{ext} components (R_{ov}, R_{spr}) when ρ_c is reduced to $5x10^{-9}$ Ω-cm^2 (the 16nm-node target value).

doping concentrations is responsible for the sharp increase in contact resistivity with silicide depth.

Fig. 7 demonstrates specific contact resistivity projection as a function of active doping level and SBH resulted from calibrated D-D model. 2010 updated ITRS projections for ρ_c are inserted [6]. Specific contact resistivity projections, as a function of active doping level and SBH, suggest required activation levels to support ITRS projections for ρ_c in future technologies [6] for both midgap silicide and low-barrier silicide scenarios. It should be noted from Fig. 7 that a ρ_c near or below the 22nm node target of 10^{-8} Ω-cm^2, is possible via the combination of midgap silicide chemistry and high temperature, millisecond anneal (e.g., LSA, flash) [7]. Low-barrier silicide or SBH reduction engineering (e.g., $ErSi_2$ or Pd_2Si [1]), in conjunction with a high activation process, are indicated for the 16nm-node and beyond.

NFET R_{ext} component extraction is performed by examining the electron quasi-Fermi potential distribution based on calibrated 20nm bulk CMOS TCAD simulation. Fig. 8(a) illustrates the electron quasi-Fermi potential distributions at the linear operation with the same gate over-drive condition showing different potential drop near silicide contact depending on contact resistivity modeling. R_{ext} component breakdown estimated by electron quasi-Fermi potential drop along the horizontal cut of channel and S/D region is demonstrated in Fig 8(b). The breakdown of NFET R_{ext} components, using electron quasi-Fermi potential distribution analysis indicates that i) R_{co} employing D-D contact model exhibits ρ_c near $1x10^{-8}$ Ω-cm^2 and ii) R_{co} is dominant component in R_{ext} which become comparable to other R_{ext} components (R_{ov}, R_{spr}) when ρ_c is reduced to ~$5x10^{-9}$ Ω-cm^2 level of 16nm-node target value.

V. Conclusion

A doping-dependent Schottky contact model is successfully correlated to experimental active doping levels at the silicide interface, using a novel nano-contact test structure combined with 3D simulation, for the first time. Sophisticated contact modeling is demonstrated to be a key requirement for accurate simulation of contact resistance behavior. Activation level requirements for mid-gap and low-barrier silicide contact cases are outlined for future, sub-10nm CMOS technologies.

Acknowledgment

The authors would like to thank Dr. P. Oldiges for the helpful discussion and technical support.

References

[1] R. Kuroda,H. Tanaka, Y. Nakao, A. Teramoto, N. Miyamoto, S. Sugawa, T. Ohmi, "Ultra-low series resistance W/ErSi2/n+-Si and W/Pd2Si/p+-Si S/D electrodes for advanced CMOS platform," Tech. Dig. of International Electron Device Meeting (IEDM2010), 2010, pp.580-583.

[2] S.-D. Kim, S. Jain, H. Rhee, A. Scholze, M. Yu, S.C. Lee, S. Furkay, M. Zorzi, F. Bufle, and A.Erlebach, "Modeling Gate-Pitch Scaling Impact on Stress-Induced Mobility and External Resistance for 20nm-node MOSFETs," SISPAD 2010, 2010, pp. 79-82.

[3] K. Ohuchi, C. Lavoie, C. Murray, C. D'Emic, I. Lauer, J. O. Chu, B. Yang, P. Besser, L. Gignac, J. Bruley, G.U. Singco, F. Pagette, A.W. Topol, M.J. Rooks, J.J. Bucchignano, V. Narayanan, M. Khare, M. Takayanagi, K. Ishimaru, D.-G. Park, G. Shahidi, P. Solomon, "Extendibility of NiPt silicide conatact for CMOS technology demonstrated to the 22-nm Node," Tech. Dig. of International Electron Device Meeting (IEDM2007), 2007, pp.1029 – 1031.

[4] Sentaurus TCAD Tools, Synopsys, Inc.

[5] H. Iwai, T. Ohkuro, S.-I. Ohmi, "NiSi salicide technology for scaled CMOS," Microelectronic Engineering, 2002, pp.157-169.

[6] ITRS ITRS 2010 update, [on line] http://public.itrs.net.

[7] B. Adams, D. Jennings, K. Ma, A.J. Mayur, S. Moffatt, S.G. Nagy, V. Parihar, "Chariterization of nickel silicides produced by millisecond anneal," Int. Conf. RTP, 2007, p155-160.